Journal of Additive Manufacturing Technologies
DOI: 10.18416/JAMTECH.2111591

Infinite Science | Publishing

Influence of laser energy density on geometrical forms produced by laser metal deposition of PH 13-8 Mo stainless steel

T. Muslim[1*], T. Karagoz[1], O. Yilmaz[2], M. Kas[2] and R. Ozkok[1]

[1] Coşkunöz Holding, Bursa, Turkey
[2] Advanced Manufacturing Technologies Research Group (AMTRG), Gazi University, 06570, Maltepe, Ankara, Turkey
[*] Corresponding author, email: tmuslim@coskunoz.com.tr

Abstract

Additive manufacturing (AM) is getting more popular in many industries due to direct manufacturing facilities, design flexibility and effective lead time. Directed energy deposition (DED) is a variation of AM and laser metal deposition (LMD) is regarded as a DED process and it uses laser as a heat source to melt and deposit the raw material fed through a nozzle in the powder form. This paper presents a research work that investigates the forms of laser metal deposited parts in S-shaped using PH 13-8 Mo stainless steel powders. Experimental work was conducted to produce S-shaped single bead walls with main process parameters affecting the energy density. The results have been discussed by considering the energy density levels as low, medium and high. It is clear to observe that the low energy density level parameters produce no or improper S-shaped walls. However, high energy density level parameters produce relatively well deposited walls but the geometrical forms of the walls are not steady due to heat accumulation during the deposition. Balling on the deposited walls can be seen in each energy density level. This defect occurs when there is insufficient heat energy to melt and deposit the powder from the moving nozzle.

Keywords: Additive manufacturing, Laser metal deposition, PH 13-8 Mo stainless steel

1. Introduction

Additive Manufacturing (AM) is an advanced manufacturing technology, used for the production of three-dimensional objects directly from the 3D CAD model. The material is added layer upon layer until the net or near net shaped object is created [1]. The additive manufacturing processes can be classified into seven categories as VAT Photopolymerisation, Material Jetting, Binder Jetting, Material Extrusion, Powder Bed Fusion, Sheet Lamination, and Directed Energy Deposition [2]. One of the processes that fall under the category of Directed Energy Deposition is Laser Metal Deposition (LMD). Laser is used as a heat source whereas powder or wire can be used as feedstock. The heat from the laser beam melts the substrate and creates a melt pool. At the same time feedstock in form of wire or powder is fed directly into the melt pool. The feedstock melts and forms a fusion bonded deposit on the substrate according to the 3D CAD model data. To prevent oxidation of the melt pool, inert gas such as argon is used to shield the melt pool [3]. LMD is used for various purposes including repair applications, surface coating, manufacturing near-net shaped objects and fabricating functionally graded materials [4]. The final quality of the near net shaped object manufactured via LMD is greatly influenced by the process parameters. The critical process parameters for the LMD process include laser power, scan velocity, powder feed rate, shielding gas flow rate, laser spot diameters and percentage overlapping between single tracks.

Precipitation hardening stainless steels (PH SS) were first systematically used during World War II when US Steel launched “Stainless W” (UNS S 17600) [5]. They are a family of corrosion-resistant alloys [6] and they have higher strength than austenitic or ferritic stainless steels [7]. PH 13-8 Mo stainless steel is a martensitic precipitation/age-hardening stainless steel with high strength and hardness, good ductility and toughness and excellent resistance to corrosion [8]. The hardening occurs due to the precipitation of β-NiAl precipitates during the precipitation hardening heat treatment [9]. PH 13-8 Mo stainless steel is used in a wide variety of applications such as nuclear reactor components, landing gear parts, cold-headed and machined fasteners, shafts, valve parts, petro-chemical applications and, various aircraft components [8].

Sun et al. [10] investigated the influence of process parameters (laser power, scan velocity and powder feed rate) on the cladding bead geometry (height, width and depth) for Ti-6AL-4V powder. A mathematical model was developed based on Central composite design (CCD) and response surface methodology (RSM). The relationship between the process parameters, and the response variables was analyzed. It was found that powder feed rate is the dominant factor on the width and height of the clad. The scan velocity has the strongest effect on the penetration into the substrate. Masaylo et al. [11] studied how the quality of cladding can be improved, by changing the process parameters (laser power, scan velocity, powder feed rate, hatch spacing, vertical head lift). Process defects were identified, based on the source of origin (feedstock powder, improper scan strategy, excessive/insufficient energy density). The article proposes strategies to avoid process-induced defects. In the same way, Liu et al. [12] analyzed the influence of energy density on geometrical characteristics, microstructure, and mechanical properties of Inconel 718 parts manufactured by laser engineered net shaping (LENS). Block and thin wall specimens were deposited using 25 different energy densities. The evaluated properties evaluated include part dimensional shrinkage, surface roughness, surface hardness, and microstructure (dilution, porosity, grain size, dendritic arm spacing). It was found that the energy density has a significant effect on the surface roughness, part shrinkage, and porosity for as-deposited Inconel 718 parts fabricated via LENS. Energy density window with optimum properties is proposed.

This study aims to investigate the influence of the most influential process parameter which is laser energy density (J/mm^3) on the quality and shape of the deposits produced by laser metal deposition using PH 13-8 Mo powder material.

2. Material and methods

The conducted experimental works was carried out using Erlaser Hard + Clad machine developed by Erlas, Germany. The system consists of a co-axial powder nozzle attached to a 6-axes robot (Kuka Kr 90). Fibre-coupled high power diode laser (Laserline LDF 4000 – 100) with a maximum power of 4.0 kW was used. Argon was used as the shielding gas. The working distance between the nozzle and the work piece was 12mm. The laser spot size in diameter was fixed at 3.5mm. The LMD setup for additive manufacturing trials is depicted in Fig. 1. Gas atomized PH 13-8 Mo stainless steel powder of particle size 45-150 μm supplied by Sandvik Osprey Ltd, UK is used in the experimental works. 1050 stainless steel was used as the substrate material. Two substrates of size (51cm x 9cm x 4cm) were used. Argon was used as a carrier gas to transport the powder from the hopper to the nozzle. Table 1 shows the elemental composition of the powder.

Table 1. Composition of PH 13-8 Mo Stainless Steel

Element	Composition (%)
Cr	11.8
Ni	9.3
Mo	1.56
Al	1.43
Mn	0.3
Si	0.19
C	0.017
Fe	Balance

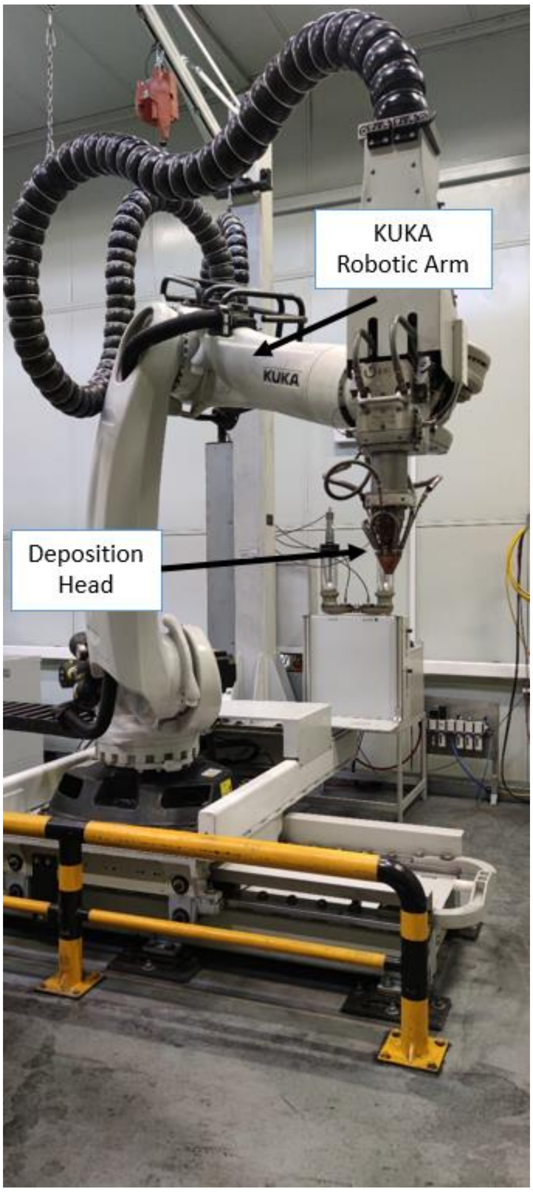

Fig 1. Robotic LMD system with co-axial powder nozzle and the accessories.

Taguchi technique was adopted to determine the process parameter combination when designing the experiments. In this study, laser power, scan velocity, powder feedrate and gas flow rate are used as variable input process parameters. The process parameters were generated using the setting in Table 2.

Table 2. Input process parameters and their levels.

SI. No.	Parameter	Level 1	2	3	4	5
1	Laser power (W)	600	800	1000	1200	1500
2	Scan Velocity (m/s)	6	8	10	12	15
3	Powder federate (rev/min)	2.5	3	3.5	4	4.5
4	Gas flow rate (ltr/min)	1	3	5	7	9

Journal of Additive Manufacturing Technologies
DOI: 10.18416/JAMTECH.2111591

The settings were entered in to the Minitab Software® and it generated a set of process parameters (see Table 3). Energy density, E (J/mm^3) is a variable that is used to quantify energy delivered per unit volume of the material. It is calculated using equation (1) [13].

$$E = \frac{P}{V_{beam}\,\pi {r_b}^2} \qquad (1)$$

Where

- P, Laser power, (W)
- r_b = Spot radius (mm)
- V_{beam} = Scan velocity (mm/s)

A specifically designed S-shaped single bead walls with 20 layers was deposited for each set of process parameters. Fig. 2 shows the 3D CAD model of the S-shaped models on a single substrate.

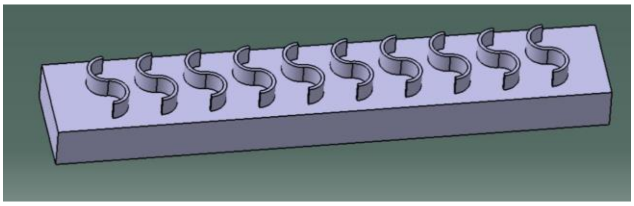

Fig 2. 3D CAD model for the S shape.

The deposition direction was unidirectional. The coupons were deposited with a dwell time of one minute after the initial 10 layers. Post deposition, heights were measured at 5 equidistant points and averaged out for each geometrical form. Table 3 shows the average heights. The heights were measured using INSIZE electronic caliper of model G0091.

3. Results and discussion

After depositing the S-shaped walls, certain deposited S-walls did not build up at all. However, some of them were successfully build up. Fig. 3 shows all the deposited S-shaped single bead walls. Energy density is the most influential factor in melting based additive manufacturing processes, such as laser/electron beam powder bed fusion processes, laser metal deposition, wire arc additive manufacturing etc. Energy density is very critical for material deposition/melting and must be chosen effectively.

Table 4 shows energy densities (specific energy) grouped into three categories based on the deposited material geometrical properties. LMD trials with low energy densities produced no or improper S geometries as shown in Fig.4. Energy density is the main factor that influences the melting of the powder, deposit dimensions, dilution and surface roughness. Low energy density produces less heat energy necessary to melt the powder properly. No proper geometries were seen in Exp No 3, 4, 5 because of very low energy densities. The higher scan velocity and relatively lower laser power in Exp no 9 and 2 caused the balling defect. Table 4 shows the average deposition heights for low, medium and high energy densities. Due to improper energy density to melt the fed powder, the average deposition height for low energy density trials is 3.62mm.

Table 3. Design of experiments.

Sample No	Laser Power (W)	Scan Velocity (mm/s)	Powder feedrate (rev/min)	Gas flow rate (liters/min)	Laser Energy density (J/mm³)	Average Height (mm)
1	600	6	2,5	1	10,39	9,64
2	600	8	3	3	7,80	8,98
3	600	10	3,5	5	6,24	0,00
4	600	12	4	7	5,20	0,00
5	600	15	4,5	9	4,16	0,00
6	800	6	3	5	13,86	13,95
7	800	8	3,5	7	10,39	11,28
8	800	10	4	9	8,32	9,73
9	800	12	4,5	1	6,93	9,19
10	800	15	2,5	3	5,54	3,07
11	1000	6	3,5	9	17,32	20,58
12	1000	8	4	1	12,99	13,78
13	1000	10	4,5	3	10,39	13,21
14	1000	12	2,5	5	8,66	4,47
15	1000	15	3	7	6,93	4,15
16	1200	6	4	3	20,79	19,47
17	1200	8	4,5	5	15,59	17,33
18	1200	10	2,5	7	12,47	4,87
19	1200	12	3	9	10,39	5,50
20	1200	15	3,5	1	8,32	5,15
21	1500	6	4,5	7	25,98	22,48
22	1500	8	2,5	9	19,49	6,91
23	1500	10	3	1	15,59	6,69
24	1500	12	3,5	3	12,99	6,55
25	1500	15	4	5	10,39	6,47

Fig 3. S shaped deposits of PH 13-8 Mo Stainless steel on 1050 Stainless steel substrate.

Table 4. Laser energy density categorization matrix.

No	Laser Energy density (J/mm³)	Category	Average Height (mm)
1	0-7.99	Low	3,62
2	8-12.99	Medium	8,24
3	13 and above	High	15,34

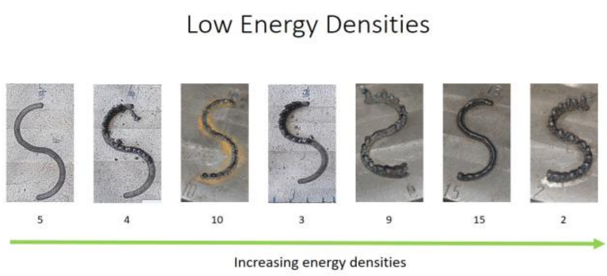

Fig 4. S shaped deposits with low energy densities.

Medium energy densities produced visible S-shaped walls. Fig. 5 shows S-shaped walls deposited with medium energy densities. Balling defect is observed in Exp. No 1, 7 and 8 due to lower laser power and higher scan velocity. However, other trials were completed with good geometrical shapes. The edge effect is observed on the deposits with a peak at the deposition start and a slope towards the end of the deposit. This is because of the uncontrolled robot speed. The robot starts from zero velocity and accelerates in the beginning, and towards the end, it decelerates to zero velocity. The accelerations and decelerations contribute to the edge effect and should be optimized. The average height of the deposited walls is higher than the low energy density results. The average deposition height for medium energy density trials is 8.24mm since more material is melted and deposited during the process due to the sufficient energy density necessary for deposited material.

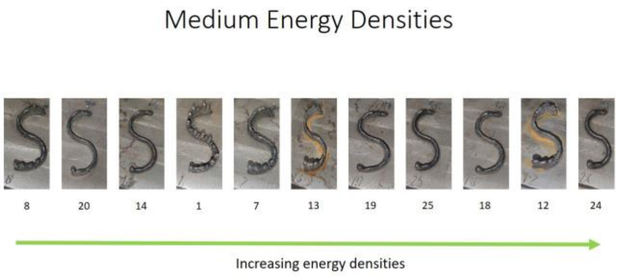

Fig 5. S shaped with medium energy densities.

Higher energy densities produced taller S-shaped walls because of increased deposition rates. High energy densities were obtained with higher laser power and lower scan velocity. Good deposition rates were obtained since more material was melted and deposited. High energy densities lead to more heat input during the deposition process. This results in heat accumulation layer upon layer as the wall grows. It can be good for increasing deposition rates. However, heat accumulation can influence the microstructure/ mechanical properties of the deposit, causing unwanted defects such as porosity/cracks, and increased residual stresses making the deposit prone to distortion. With heat accumulation, the temperature of the deposit, as well as the substrate, will increase at the same time. This makes it impossible to control the form of the part shape due to the fluidity of the deposition. Fig. 6 shows improper geometries with Exp.no 17, 11, 16 and 21. When the deposited height is considered, the average height measured of the walls is relatively higher than the low and medium energy density experiment results. It is measured as 15.34mm which is almost triple and double compared to low and medium energy density results. This is because the higher energy density produces more heat concentrated on the melt pool area and more powder is melted and eventually more material is deposited.

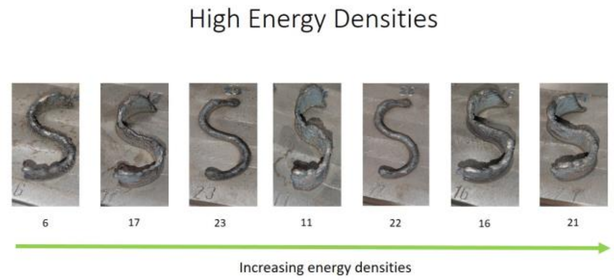

Fig 6. S shaped deposits with high energy densities

4. Conclusions

Laser metal deposition is a highly effective AM method to produce large, dense and structural parts. The presented work investigates the most critical process parameters (laser power and scan velocity) which affect the geometrical forms of deposited parts. The following conclusions are highlighted;

- Energy density is directly related to laser power, laser spot size and scan velocity.

- Heat input necessary for melting and depositing the raw material in LMD is affecting the geometrical form of the deposited part.

- Low energy density level parameters produce no or improper depositions.

- Higher energy densities produce relatively high walls but improper geometries which can be formed due to heat accumulation.

- Balling effect is obvious when disproportionate laser power and scan speed is applied.

- Depending on the energy density levels, the maximum average height is measured on higher energy density trials and gradually lower height is obtained for medium and low energy density trials.

Acknowledgments

We would like to thank TUBITAK and Coşkunöz Holding about their contribution to 2244 Industrial Doctorate Programme. We also would like to gratitude TUBITAK Eureka, Eureka Smart Cluster and Coşkunöz Holding for their support for REMEDI Project under grant No 9190007.

Author's statement

Conflict of interest: Authors state no conflict of interest. Informed consent: Informed consent has been obtained from all individuals included in this study. Ethical approval: The research related to human use complies with all the relevant national regulations, institutional policies and was performed in accordance with the tenets of the Helsinki Declaration, and has been approved by the authors' institutional review board or equivalent committee.

References

1. "What Is Additive Manufacturing? Definition and Processes." TWI, www.twi-global.com/technical-knowledge/faqs/what-is-additive-manufacturing. Accessed 5 July 2021.

2. ISO / ASTM52900-15, Standard Terminology for Additive Manufacturing – General Principles – Terminology, ASTM International, West Conshohocken, PA, 2015, www.astm.org
3. Gu, D. D., et al. "Laser Additive Manufacturing of Metallic Components: Materials, Processes and Mechanisms." International Materials Reviews, vol. 57, no. 3, 2012, pp. 133–64. Crossref, doi:10.1179/1743280411y.0000000014.
4. Dinda, G. P., et al. "Laser Aided Direct Metal Deposition of Inconel 625 Superalloy: Microstructural Evolution and Thermal Stability." Materials Science and Engineering: A, vol. 509, no. 1–2, 2009, pp. 98–104. Crossref, doi:10.1016/j.msea.2009.01.009.
5. "Precipitation Hardened Stainless Steels — Sandvik Materials Technology." Materials Sandvik, www.materials.sandvik/en/materials-center/expert-columns/archive/2018/02/precipitation-hardened-stainless-steels. Accessed 7 July 2021.
6. "Precipitation Hardening Stainless Steels." TWI, www.twi-global.com/technical-knowledge/job-knowledge/precipitation-hardening-stainless-steels-102. Accessed 7 July 2021.
7. Kazior, Jan, et al. "Properties of Precipitation Hardening 17–4 PH Stainless Steel Manufactured by Powder Metallurgy Technology." Advanced Materials Research, vol. 811, 2013, pp. 87–92. Crossref, doi:10.4028/www.scientific.net/amr.811.87.
8. "13–8 Mo Tech Data." High Temp Metals, www.hightempmetals.com/techdata/hitemp13-8MOdata.php. Accessed 7 July 2021.
9. Seetharaman, V., et al. "Precipitation Hardening in a PH 13–8 Mo Stainless Steel." Materials Science and Engineering, vol. 47, no. 1, 1981, pp. 1–11. Crossref, doi:10.1016/0025-5416(81)90034-3.
10. Sun, Yuwen, and Mingzhong Hao. "Statistical Analysis and Optimization of Process Parameters in Ti6Al4V Laser Cladding Using Nd: YAG Laser." Optics and Lasers in Engineering, vol. 50, no. 7, 2012, pp. 985–95. Crossref, doi:10.1016/j.optlaseng.2012.01.018.
11. Masaylo, D., et al. "Effect of Process Parameters on Defects in Large Scale Components Manufactured by Direct Laser Deposition." Materials Today: Proceedings, vol. 30, 2020, pp. 665–71. Crossref, doi:10.1016/j.matpr.2020.01.519.
12. Liu, Zhichao, et al. "Influence of Energy Density on Macro/Micro Structures and Mechanical Properties of as-Deposited Inconel 718 Parts Fabricated by Laser Engineered Net Shaping." Journal of Manufacturing Processes, vol. 42, 2019, pp. 96–105. Crossref, doi:10.1016/j.jmapro.2019.04.020.
13. Thompson, Scott M., et al. "An Overview of Direct Laser Deposition for Additive Manufacturing; Part I: Transport Phenomena, Modeling and Diagnostics." Additive Manufacturing, vol. 8, 2015, pp. 36–62. Crossref, doi:10.1016/j.addma.2015.07.001.